Discovering More Mathematics and Applications by Integrating CAS with 3D DGS

Wei-Chi YANG
wyang@radford.edu
Department of Mathematics
and Statistics
Radford University
Radford, VA 24142
USA

Abstract

It is known that Computer Algebra Systems such as Maple [9], Mathematica [10] and etc. have assisted us greatly in numeric, algebraic and symbolic computations, which are pivotal for our teaching, learning and research. We have also seen the impacts of 2D Dynamic Geometry Software (DGS) such as Geometers' SketchPad [11], Cabri II [12] and etc in mathematics education . In this paper, we use examples to demonstrate, from users' point of view, how the integration of CAS with a 3D DGS provides us crucial 3D visualizations and theoretical verification needed in teaching and research in mathematics and its applicable fields.

1 Introduction

It is often the case that research and applications in mathematical fields are originated from real-life problems. In this paper, we demonstrate with the evolving technological tools, it is also possible to link our mathematics discoveries to areas such as in sciences, technology and engineering. We emphasize the importance of recognizing technological tools as research options. We make our examples accessible to those who have mathematics knowledge up to university level. Invest in mathematics teaching and research in higher education is essential for cultivating students' innovation and creative thinking skills. While professional trainings in the area of content knowledge for secondary schools (middle or high schools) are important. It is equally important that we promote exploratory activities which allow students to think and solve problems creatively in university levels and beyond. We select some examples to demonstrate how technological tools allow us exploring problems from 2D to 3D and beyond, which shows that the content can be chosen *continuously* going from middle, high schools to undergraduate and graduate schools. The examples will show how different topics or concepts that students have encountered in the past can be *connected*, which could link mathematics to physics or applied sciences. Finally learners will discover how technological tools can expand their mathematics knowledge and promote their *creative* thinking skills.

In current technological era, students are exposed to solving problems with various software packages. Consequently, teachers and educators need to update themselves in seeking and designing proper sets of problems where mathematics knowledge can be integrated in interdisciplinary areas. A sound mathematics curricula should include component where exploration is cultivated and encouraged. In particular, we observe the following areas where technological tools have become indispensable and have assisted us greatly in teaching, learning and research.

1. The capability of performing graphic, algebraic, numeric and symbolic representations within a CAS helps us not only for making educational conjectures but also verifying theoretical proofs.

2. The capability of constructing multiple 2D or 3D figures within a 2D or 3D DGS allows us conjecture if our 2D observations can be extended to ones in 3D. Some 2D or 3D scenarios provide us crucial conjectures before theories can be formed and verified using a CAS.

3. Once learners understand fully how a 3D scenario works with the help from CAS and DGS, they can generalize the theories to finite dimensions or beyond. For example, the integration of multivariable calculus and linear algebra, with the help of technologies, will inspire students to investigate area such as differential geometry. In this paper, we give some examples to show why the integration of a CAS and a 3D DGS is crucial for teaching, learning and research in mathematics.

2 Extend from 2D to 3D or higher if possible

By seeing the pictures shown in Figure 1(a), one may recall the Mean Value Theorem (MVT). If we apply the Mean Value Theorem on a parametric curve, we obtain the Cauchy Mean Value Theorem as mentioned in [6] , which we illustrate simply using Figure 1(b). We state the MVT roughly as follows:: Given the blue smooth curve C (or the one resembles a higher parabola opening down) in an interval containing the line segment AB, there should exist a point P on C so that the tangent line is parallel to AB. We note that it is identical to finding the place where we have horizontal tangent on the new green curve C'(or the one resembling lower parabola opening down in Figure 1(a)). In other words, the $x-coordinate$ for which the Rolle's Theorem holds for the green curve is the same as the place where the MVT holds for the blue. Same conclusion can be drawn for CMVT, see Figure 1(b). In [6], we used geometric approaches to see how we can construct new functions where we may apply Rolle's Theorem when proving

MVT and CMVT respectively.

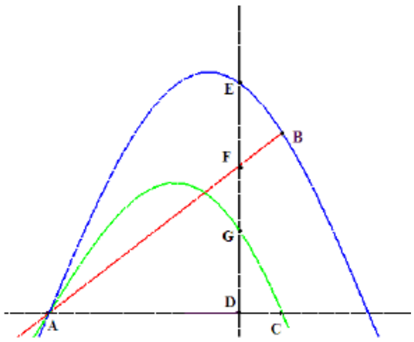

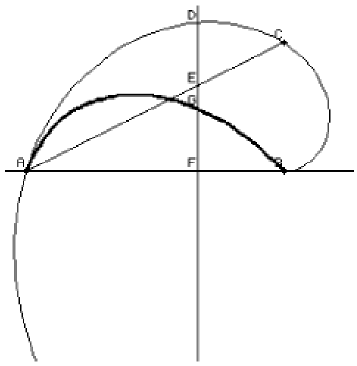

Figures 1(a) Picture for a Mean Value Theorem

1(b) Picture for a Cauchy Mean Value Theorem

As mentioned in [2], we can extend the statements and proofs of MVT and CMVT to higher dimensions, which we demonstrate these effects in Figures 2(a) and 2(b) below. Intuitively, if a plane intersects a smooth surface, then we can find a point on the surface where its tangent plane is in the same direction as the given plane. *In [2], we extended the ideas found in 2D and used geometric approaches to see how we can construct new functions where we may apply Rolle's Theorem when proving MVT and CMVT respectively.*

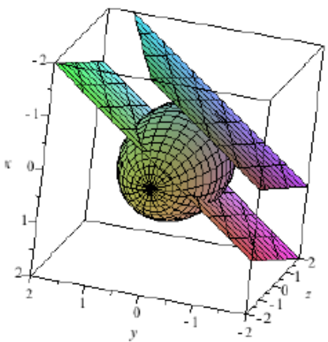

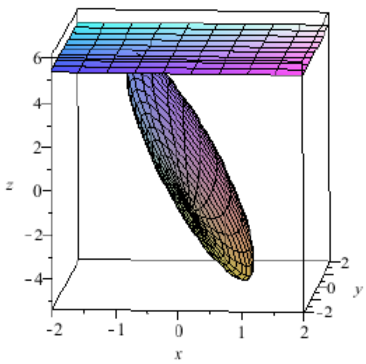

Figure 2(a) MVT for a plane

Figure 2(b) MVT and horizontal tangent

Next we start with two intersecting surfaces (say an ellipsoid and a paraboloid) as we can see in Figure 3(a). If we fix the given ellipsoid, and move the paraboloid only vertically (in this case; more details will be given later), we would like to find a place where both surfaces are tangent to each other. Intuitively, we expect two solutions, and we describe them as follows:

Example 1 *We fix an ellipsoid of the form $g(x,y,z) = x^2/a^2 + y^2/b^2 + z^2/c^2 = 0$, where a, b, and c are real numbers, and we consider the level surfaces for $f(x,y,z) = z - mx^2 - ny^2$, where m and n are two given positive real numbers. The higher dimension Mean Value Theorem* *in this case (see [2]) can be interpreted as follows: If these two surfaces intersect, then there exists a point* (x_0, y_0, z_0) *where the paraboloid touches the ellipsoid. Mathematically, we are looking for a constant* k*, and the point* (x_0, y_0, z_0) *where* $f(x_0, y_0, z_0) = k$ *and* $g(x_0, y_0, z_0) = 0$ *are tangent to each other. In other words, we are looking for a constant* λ *so that the gradient vectors at* (x_0, y_0, z_0) *for these two surfaces are parallel to each other or the condition* $\nabla f(x_0, y_0, z_0) = \lambda \nabla g(x_0, y_0, z_0)$*, is met. As described in [2], we use a CAS such as Maple to solve a set of equations due to the Lagrange multiplier method and reach a set of numeric solutions if the values of* $a, b, c,$ m *and* n *are given first.* ***However if we were to show each correct answer for different*** $a, b, c,$ m ***and*** n***, we need to substitute numeric values into Maple each time to generate an individual graph.*** *In such case, a dynamic geometry 3D software such as GInMA [6] is appreciated and helpful. The GInMA can take symbolic possibilities into considerations and allow users to move the parameter* k *and see where* $f(x, y, z) = k$ *and* $g(x, y, z) = 0$ *might tangent to each other. Furthermore, the program also permits users to choose a set of parameters,* a, b, c, m *and* n *first, and see when we will have exactly two solutions. For* $m = 0.7$ *and* $n = 0.4$ *as shown in Figures (b) and (c), we can rotate the pictures properly to see where these two surfaces are tangent to each other.*

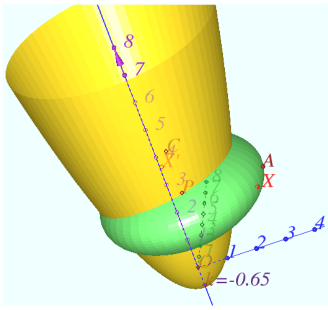

Figure 3(a) MVT-orginal

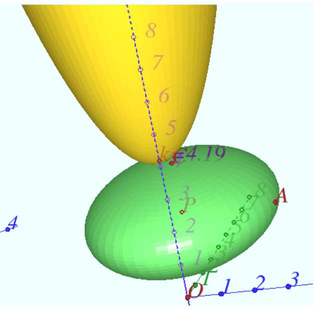

Figure 3(b) First possible solution

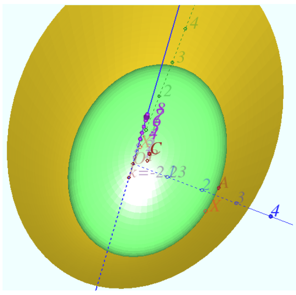

Figure 3(c) MVT-solution 2

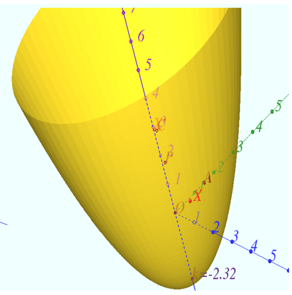

Figure 3(d) Solution 2-rotation

The example above shows there is need to integrate a CAS with a 3D DGS.

3 Creativity does not come from drills

In many mathematics education systems, college entrance examinations put a great burden for students and teachers to focus on what should be learned and taught. For example, although the twelfth five year guideline in China indicated that 'the education reform is a vital step for increasing the manpower strengthening the development of the country. Technological tools will play an important part for this integration; due to the pressure of entrance examinations, teachers often utilize the designated mathematics experimental periods for doing more drilled or rote type math problems. This is a typical situation in many examination oriented countries. If we look at some of those university entrance examination math problems, we realize that we are teaching students skills in memorization and special techniques of solving problems. As a result, we may have lost many potential students who cannot perform well in a test. Therefore, it is not difficult to conjecture that if the depth of a course in math is too deep, students may lose interests in studying mathematics early; on the other hand, using technological tools when exploring graphical representations in a math topic may inspire students' interests in learning more mathematics. In short, we need to allow students to explore problems that are not discussed in a regular textbook or at a traditional classroom. In the next example, we discuss a question that we encounter when teaching integration. For Figure 4(a), we want find the closed area bounded by a curve and a line segment, this is a situation where we need to subdivide the region into two sub-regions if we were to use typical technique of using vertical or horizontal partitions. Alternatively, we may use change of bases as mentioned in [4], to reach useful results inspired by technological tools.

Example 2 *We are given the circle of the form* $x^2 + y^2 + 2.22x - 0.1y - 0.529 = 0$ *and* $y = 0.9802 * x + 1.866$*, which we picked rather randomly to demonstrate that applying one integration is not enough using usual vertical (*dx*) or horizontal (*dy*) partitions. We intend to find the area bounded by the circle and the line as sketched in Figure 4(a). If we were to use traditional integration technique, we will need to apply integration on two parts (due to* dx *and* dy*). This is where we should apply the Riemann sum with respect to a slanted line (see Figure 4(b))*

To link our result to a Green Theorem, we first note if $\mathbf{F}(x, y) = (P(x, y), Q(x, y))$ is a vector field, $\operatorname{curl} \mathbf{F} = \begin{vmatrix} i & j & k \\ \frac{\partial}{\partial x} & \frac{\partial}{\partial y} & \frac{\partial}{\partial z} \\ P & Q & 0 \end{vmatrix} = \begin{bmatrix} 0 & 0 & \left(\frac{\partial Q}{\partial x} - \frac{\partial P}{\partial y}\right) \end{bmatrix} = \left(\frac{\partial Q}{\partial x} - \frac{\partial P}{\partial y}\right)\mathbf{k}$. Therefore, $(\operatorname{curl} \mathbf{F}) \cdot \mathbf{k} = \frac{\partial Q}{\partial x} - \frac{\partial P}{\partial y}$. We can write the Green's Theorem in the vector form below:

$$\begin{aligned} \int_C \mathbf{F} \cdot d\mathbf{r} &= \int\int_R (\operatorname{curl} \mathbf{F}) \cdot \mathbf{k} \, dA. \qquad (1) \\ &= \int\int_R \left(\frac{\partial Q}{\partial x} - \frac{\partial P}{\partial y}\right) dA = \int_C P\,dx + Q\,dy \end{aligned}$$

On the other hand, by using intuitive rotation or change of bases technique, we reach a 2D formula (as shown in [4]) which can be seen as a special cases of Green Theorem:

Theorem 3 *Let* C *be the smooth curve* $\mathbf{w}(t) = [x(t), y(t)]$*, where* $t_1 \le t \le t_2$*. Let* R *be the region bounded by* C*, the line* $y = mx + b$*, and the perpendiculars to the line from* $(x(t_1), y(t_1))$

to $(x(t_2), y(t_2))$*. We denote the counterclockwise boundary curve of* R *by* ∂R*. If* P *and* Q *are scalar fields with continuous partial derivatives satisfying* $\frac{\partial Q}{\partial x} - \frac{\partial P}{\partial y} = 1$*, then*

$$\begin{aligned} \int_C \mathbf{F} \cdot d\mathbf{r} &= \int_{\partial R} P\,dx + Q\,dy = \int\int_R \left(\frac{\partial Q}{\partial x} - \frac{\partial P}{\partial y} \right) dA \\ &= \frac{-1}{1+m^2} \int_{t_1}^{t_2} (-x(t)m + y(t) - b)\,(x'(t) + y'(t)m)\,dt, \end{aligned} \tag{2}$$

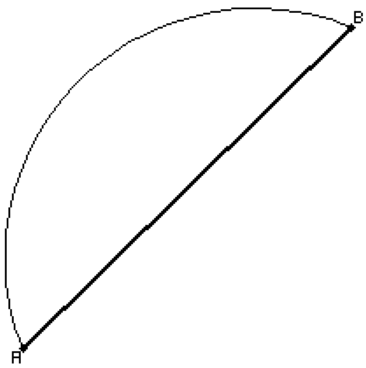

Figure 4(a) Area and a slanted line

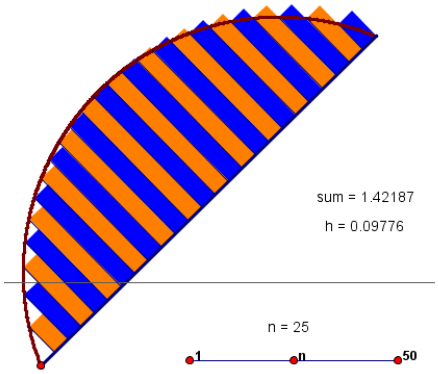

Figure 4(b) Natral partitions with respect to a slanted line

We now extend the idea of finding an area through rotation (or change of bases) to finding the volume of a solid bounded by a slanted plane and a surface in 3D analogously. As expected, it is a special case of Divergence Theorem mentioned in [4]. The detailed techniques and computation methods were described in [1] for finding the finite volume bounded by a plane and a quadratic. (See Figures 5(a), (b) and (c).) We address only few points where the integration of 3D DGS and CAS have provided us crucial intuitions while exploring the problems and refer readers for more algebraic and computational details in [1].

1. Algebraically with the help of CAS, we show the intersections between a plane and a quadric is an ellipse if there is an intersection.

2. To carry out the integration of finding the volume of a bounded solid algebraically, we properly choose the right coordinate on the cross section so that the center is at the center of the ellipse. Two eigenvectors correspond to major and minor axes for the ellipse, and the normal vector of the cross section at the center is in the same as the normal direction of the given plane.

3. We need a CAS (such as Maple) to assist us of solving and analyzing complex solutions before we incorporate the solutions into drawing them in 3D DGS (such as GInMA). Subsequently, the graphics can be made dynamic in a 3D DGS.

We discuss how we may find the volume of the region bounded by a quadric and a plane by using the Divergence theorem. We state the theorem for those who are familiar with the theorem as follows

$$\int\int\int_V \operatorname{div}\mathbf{T}dV = \int\int_S \mathbf{T}\cdot\mathbf{ds}, \tag{3}$$

where V is the solid enclosed by the surface S, $\operatorname{div}\mathbf{T}$ represents the divergence of the vector field $\mathbf{T}$, and $\mathbf{ds} = \begin{pmatrix} dydz \\ dzdx \\ dxdy \end{pmatrix}$. Intuitively, the idea is to properly choose a vector field $\mathbf{T}$ so that $\operatorname{div}\mathbf{T}$ is a constant, say $C_0 \neq 0$, and $\mathbf{T}\cdot\ \mathbf{m} = \mathbf{0}$, where $\mathbf{m}$ is the normal vector of the given plane. Therefore, we have

$$\int\int\int_V \operatorname{div}\mathbf{T}dV = C_0\int\int\int_V dV = C_0 V, \tag{4}$$

which is the volume of the bounded solid multiplied by C_0. On the other hand, since $\mathbf{T}\cdot\ \mathbf{m} = 0$, and the vector $\mathbf{ds}$ (on the plane) is collinear with $\mathbf{m}$, we see that $\int\int_{plane}\mathbf{T}\cdot\mathbf{ds} = 0$. Therefore the volume of the solid of intersection is the surface integral of $\mathbf{T}$ over the given quadric. In other words we compute the volume of the bounded solid by using the following

$$V = \frac{1}{C_0}\int\int_S \mathbf{T}\cdot\mathbf{ds}. \tag{5}$$

The computations of $\int\int_S \mathbf{T}\cdot\mathbf{ds}$ is quite technical for various quadric S. We refer readers to [1] for complete details of finding the volumes bounded by a quadric and a plane by using the Divergence Theorem.

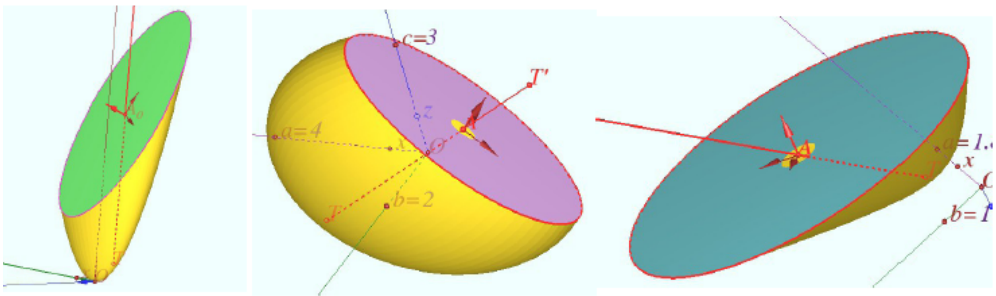

Figures 5(a), (b) and (c) Volumes bounded by a Paraboloid, Ellipsoid or Hyperboloid with two sheets and a plane

Next we may adopt the Stokes' Theorem to find the volume of a solid. The Stokes' Theorem

$$\int\int\int_V (\operatorname{curl}\mathbf{T}\cdot\mathbf{N})\,dV = \int\int_S \mathbf{T}\times\mathbf{ds} \tag{6}$$

says that the collective measure of this rotational tendency taken over the entire solid is equal to the tendency of the a fluid to circulate around the surface S. Alternatively, Stokes' Theorem says

$$\int_M d\omega = \int_{\partial M}\omega,$$

where M is an $n-$dimensional manifold with boundary ∂M, and ω is an $(n-1)$-form. Thus if $n=3$, then M is some volume V and ∂M is the surface S of V. Since

$$\omega = adxdy + bdxdz + cdydz,$$

we have

$$dw = a_z dzdxdy + b_y dydxdz + c_x dxdydz = (a_z - b_y + c_x)dxdydz,$$

where $a_z = \frac{\partial a}{\partial z}, b_y = \frac{\partial b}{\partial y}$ and $c_x = \frac{\partial c}{\partial x}$. Thus it follows from Stokes' Theorem that

$$\int_V (a_z - b_y + c_x)dxdydz = \int_S (adxdy + bdxdz + cdydz).$$

If $\mathbf{T} = (a,b,c)$ is a vector field, then curl $\mathbf{T}$ $=\nabla \times \mathbf{T} = (c_y - b_z, a_z - c_x, b_x - a_y)$. If we set

$$\eta = -cdxdz - bdxdy, \theta = adxdy - cdydz, \omega = bdydz + adxdz,$$

then

$$\begin{aligned} d\eta &= -c_y dydxdz - b_z dzdxdy = (c_y - b_z)\, dxdydz, \\ d\theta &= a_z dzdxdy - c_x dxdydz = (a_z - c_x)\, dxdydz, \\ d\omega &= b_x dxdydz + a_y dydxdz = (b_x - a_y)\, dxdydz, \end{aligned}$$

we see that

$$(\nabla \times \mathbf{T})\, dxdydz = (d\eta, d\theta, d\omega).$$

On the other hand, if $\mathbf{ds} = (-dydz, dxdz, -dxdy)$, then it is easy to see that

$$\mathbf{T} \times \mathbf{ds} = (\eta, \theta, \omega),$$

we note

$$\begin{vmatrix} i & j & k \\ a & b & c \\ -dydz & dxdz & -dxdy \end{vmatrix} = (-bdxdy - cdxdz, -cdydz + adxdy, adxdz + bdydz).$$

Hence

$$\int_M (\nabla \times \mathbf{T})\, dxdydz = \int_V (d\eta, d\theta, d\omega) = \int_S (\eta, \theta, \omega) = \int_S \mathbf{T} \times \mathbf{ds}. \tag{7}$$

To figure out the volume M, it follows from equations (6) or (7) that we need to properly select a vector field $\mathbf{T}$ so that curl $\mathbf{T}$ or $\nabla \times \mathbf{T}$ is a constant and we use only one component of $\nabla \times \mathbf{T}$ in equation (7) to compute the needed volume. We refer readers [1] for details of finding the volumes bounded by a plane and a quadric using the Stokes' Theorem.

4 Geometric constructions are crucial for 2D and 3D

In the following two examples, we show how solutions obtained from geometric construction, with a 2D or 3D DGS, are identical with those obtained analytically, algebraically and numerically with a CAS. First we consider the shortest total distance problem: We are given three disjoint curves, C_1, C_2, and C_3. We want to find points A, B and D on the curves C_1, C_2, and C_3 respectively so that the total distance of $AB + AD$ is the smallest. To be precise, we use the following example that is described in [5]. We use the total square distance $AB^2 + AD^2$ in our discussion thereafter.

Example 4 *Let*

$$\begin{aligned} g_1(x_1, y_1) &= \sin x_1 - y_1 \\ g_2(x_2, y_2) &= x_2^2 - y_2 + 2 \\ g_3(x_3, y_3) &= (x_3 - 3)^2 + (y_3 - 3)^2 - 1 \end{aligned}$$

and we are given three disjoint curves, C_1, C_2, and C_3 given by $g_1(x_1, y_1) = 0$, $g_2(x_2, y_2) = 0$ and $g_3(x_3, y_3) = 0$ respectively. We would like to find the shortest total distance from C_1 to C_2 and C_1 to C_3 in the closed and bounded set of $[-2, 5] \times [-1, 4]$. We show the curves C_1, C_2, and C_3 in Figure 6 below.

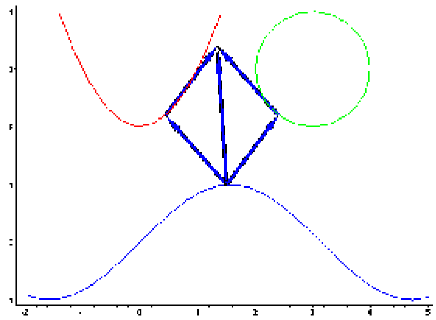

Figure 6. Linear combination in 2D

Method 1 (CAS Algebraic and Numeric Solution): As described in [5], we may solve this problem by using Lagrange multipliers method. For example, if we write $\mathbf{x}_i = (x_i, y_i), i = 1, 2, 3$, our objective is to minimize the total square distance

$$\begin{aligned} f(\mathbf{x}_1, \mathbf{x}_2, \mathbf{x}_3) &= \|\mathbf{x}_1 - \mathbf{x}_2\| + \|\mathbf{x}_1 - \mathbf{x}_3\| \\ \text{subject to } g_1(\mathbf{x}_1) &= 0, g_2(\mathbf{x}_2) = 0 \text{ and } g_3(\mathbf{x}_3) = 0, \text{ or} \\ f(x_1, y_1, x_2, y_2, x_3, y_3) &= (x_1 - x_2)^2 + (x_1 - x_3)^2 + (y_1 - y_2)^2 + (y_1 - y_3)^2 \\ \text{subject to } g_1(x_1, y_1) &= 0, g_2(x_2, y_2) = 0 \text{ and } g_3(x_3, y_3) = 0. \end{aligned} \tag{8}$$

In short, if we achieve the minimum total square distance for f, it is a **necessary condition** that we find $\mathbf{x}_0 = (\mathbf{x}_1^*, \mathbf{x}_2^*, \mathbf{x}_3^*)$ and express the gradient vector,∇g_1 at a point is a linear combination of the the other two gradients, in other words,

$$\nabla g_1(\mathbf{x}_1^*) = -\frac{\lambda_2}{\lambda_1} \nabla g_2(\mathbf{x}_2^*) - -\frac{\lambda_3}{\lambda_1} \nabla g_3(\mathbf{x}_3^*), \tag{9}$$

where $\lambda_1 \neq 0$. We show the result we obtained from a CAS (Maple) below. We obtain the shortest total distance occurs when

$$
\begin{aligned}
A &= \begin{bmatrix} x_1 \\ y_1 \end{bmatrix} = \begin{bmatrix} 1.503078740 \\ .9977080403 \end{bmatrix} \in C_1, \\
B &= \begin{bmatrix} x_2 \\ y_2 \end{bmatrix} = \begin{bmatrix} .4425626436 \\ 2.195861693 \end{bmatrix} \in C_2, \\
D &= \begin{bmatrix} x_3 \\ y_3 \end{bmatrix} = \begin{bmatrix} 2.401228926 \\ 2.199079779 \end{bmatrix} \in C_3, \\
\text{and } \begin{bmatrix} \lambda_1 \\ \lambda_2 \\ \lambda_3 \end{bmatrix} &= \begin{bmatrix} -4.799050783 \\ 2.396307306 \\ 1.499989270 \end{bmatrix}.
\end{aligned}
$$

It follows from our computation that indeed $\lambda_1 \left(\nabla g_1 |_{\text{at } A} \right) = \lambda_2 \overrightarrow{AB} + \lambda_3 \overrightarrow{AC}$, which can be shown in Figure 6.

Method 2 (DGS Geometric Solution):

1. First we arbitrarily pick a point A, B' and D' on C_1, C_2 and C_3 respectively, and we total the distance $AB' + AD'$.

2. We next find points B and D on C_2 and C_3 respectively such that AB and AD are perpendicular to the tangent lines at B and D respectively.

3. We construct the normal vector at the point A, and we construct the midpoint of BD and call it E.

4. As we move A along the curve C_1, we observe that the total distance becomes the smallest when the normal vector at A passes through E. Finally if we move B' and D' toward B and D respectively, we achieve the required minimum as seen in Figure 7(c).

We see in this case the geometric interpretation coincides with the one obtained algebraically and numerically, which says that if we achieve the shortest total square distance $AB^2 + AD^2$, it is necessary that the vector $2AE$ can be written as a linear combination of AB and AD. *In other words, if E is not the midpoint of BD, then $AB + AD$ can not be the minimum.*

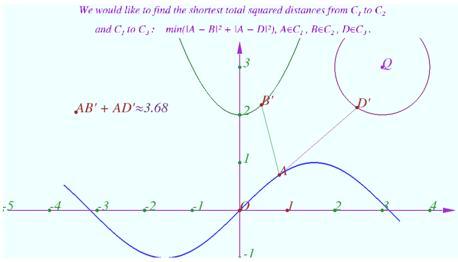

Figure 7(a) Initial geometry construction

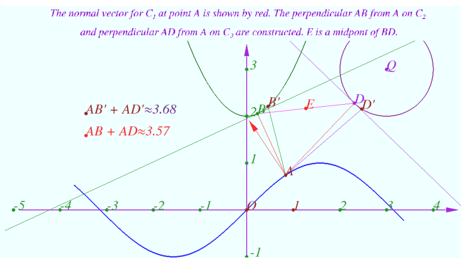

Figure 7(b) Selections of B and C

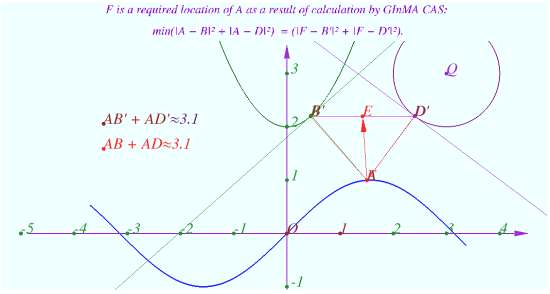

Figure 7(c) Normal vector at A and the midpoint

We extend the numerical and algebraic ideas from 2D to 3D as demonstrated in Example 6 of [5]. Here we discuss our **3D geometric construction** here:

Example 5 *We are given four disjoint convex surfaces,* S_1, S_2, S_3 *and* S_4 *given by* $g_1(x,y,z) = 0, g_2(x,y,z) = 0, g_3(x,y,z) = 0$ *and* $g_4(x,y,z) = 0$ *respectively, where*

$$\begin{aligned} g_1(x,y,z) &= x^2 + y^2 + z^2 - 1, \\ g_2(x,y,z) &= x^2 + (y-3)^2 + (z-1)^2 - 1, \\ g_3(x,y,z) &= z - (x^2 + y^2) - 2 \end{aligned}$$

and

$$\begin{aligned} g_4(x,y) = & \left(4(x-3) + (y-3) + (z-1)\right)(x-3) \\ & + \left((x-3) + 4(y-3) + (z-1)\right)(y-3) \\ & + \left((x-3) + (y-3) + 4(z-1)\right)(z-1) - 3. \end{aligned}$$

We would like to find the shortest total squared distance from S_1 *to* S_2*,* S_1 *to* S_3*,and* S_1 *to* S_4 *in the closed and bounded domain of* $[-3,4] \times [-2,5] \times [-3,5]$*. We show the surfaces* S_1 *(sphere centered at origin),* S_2 *(blue sphere or sphere away from the origin),* S_3 *(a paraboloid), and* S_4 *(an ellipsoid) in Figure 8(a).*

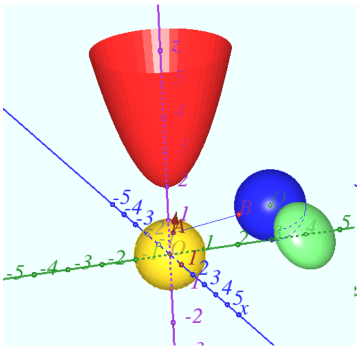

Figure 8(a) Initial stage for 3D case

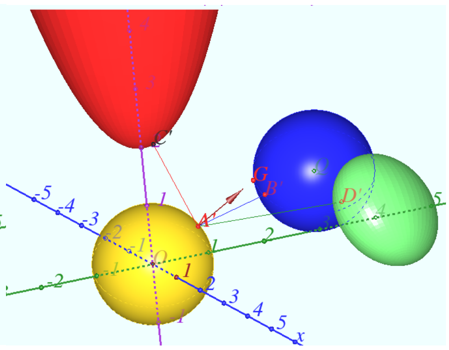

Figure 8(b) Positions of A, B, C, D *and the centroid*

1. We start with a point A on S_1, and we geometrically construct the points B, C and D on surface S_2, S_3, and S_4 respectively so that AB is perpendicular to the normal vector at B, AC is perpendicular to the normal vector at C and AD is perpendicular to the normal vector at D.

2. We next construct the centroid of BCD, which we label it as G.

3. We note that when we move the point A, the points B, C, D and G move accordingly.

4. However, we note that only when the normal vector at A passes through the centroid, G, will we obtain the shortest total square distance for $AB + AC + AD$. This can be verified by incorporating the answers obtained from Maple into GInMA ahead of time, which we label them by A', B', C' and D' on S_1, S_2, S_3, and S_4 respectively. We see minimum occurs when normal vector at A passes through G; at the same time, we should have $A = A', B = B', C = C'$ and $D = D'$.

5 Connecting mathematics to applications through technologies

If one is given a figure and any line, say $y = mx + b$, it is trivial even to a middle school student how he or she can sketch the reflection of the initial figure along the line $y = mx + b$, which we call such reflection *the general inverse with respect to the given line.* We can ask mathematically how we can find the equation of the general inverse with respect to a given line. Next, we are given a fixed point, and if the given line is a moving tangent line of a smooth curve, we ask what will be the locus of the general inverse. This can be seen as follows: If we fix a light source M and a given curve C (see Figure 9(a)), for each point A on the given curve, we can find the reflection A'' with respect to the tangent line at A. By *moving the tangent line at every point* on the curve C, the locus is called *orthotomic curve for* C. It is mentioned in [3] that the caustic curve can be viewed as the *locus of the centers of the orthotomic normals* or *the evolute of orthotomic curves.*

5.1 Obtaining orthotomic surface algebraically with a CAS

We summarize how an *orthotomic surface* can be obtained algebraically, analogous to obtaining an orthotomic curve in 2D, in the following steps:

1. We first start with finding the reflection of $(p(s,t), q(s,t), r(s,t))$ from $(x(s,t), y(s,t), z(s,t))$ with respect to a plane P passing through the origin $ax + by + cz = 0$ (we denote $\mathbf{n} = (a, b, c)$, which is the normal vector of this plane).

2. We set vector $\mathbf{v}$ to be the vector from the origin to $(x(s,t), y(s,t), z(s,t))$. We split the vector $\mathbf{v}$ into its components which are normal to the plane (denoted $\mathbf{v}_{\perp P}$) and parallel to the plane (denoted $\mathbf{v}_{\|P}$). i.e., $\mathbf{v} = \mathbf{v}_{\perp P} + \mathbf{v}_{\|P}$, we note that $\mathbf{v}_{\perp P}$ is the orthogonal projection of $\mathbf{v}$ on the normal vector $\mathbf{n} = (a, b, c)$. The reflection $\begin{bmatrix} p(s,t) \\ q(s,t) \\ r(s,t) \end{bmatrix}$ can be written as $-\mathbf{v}_{\perp P} + \mathbf{v}_{\|P} = -\mathbf{v}_{\perp P} + (\mathbf{v} - \mathbf{v}_{\perp P}) = \mathbf{v} - 2\mathbf{v}_{\perp P} = \frac{\mathbf{v}||\mathbf{n}||^2 - 2(\mathbf{v} \cdot \mathbf{n})\mathbf{n}}{||\mathbf{n}||^2}$

3. After using shifting technique, letting the original given surface S be represented by $X = \begin{bmatrix} x(s,t) \\ y(s,t) \\ z(s,t) \end{bmatrix}$ and $X_0 = (x_0, y_0, z_0)$ be on the plane $ax + by + cz = 0$. Then the reflection of S with respect to the plane $ax + by + cz = d$ can be written as

$$A\,(X - X_0) + X_0, \tag{10}$$

where $A = \frac{1}{a^2+b^2+c^2} \begin{bmatrix} -a^2+b^2+c^2 & -2ab & -2ac \\ -2ab & a^2-b^2+c^2 & -2bc \\ -2ac & -2bc & a^2+b^2-c^2 \end{bmatrix}$ is symmetric and therefore it is invertible.

4. This formula (8) can be reduced to 2D to find the general inverse with respect to a slanted line $y = mx + b$.

5. By fixing the light source M,and moving the tangent plane P^* along the given surface S, the locus of the reflection of S with respect to the all the moving tangent plane P^* is called the *orthotomic surface for* S.

6. In 2D, by taking the *locus of the centers of the curvatures of the orthotomic curve* or *the evolute of orthotomic (envelope of the orthotomic normals)*, we reach the **caustic curve** for the curve C, which is the concept from physics. Naturally, we would ask how we can define a caustic surface in 3D.

5.2 Obtaining orthotomic curve or surface geometrically with a 3D DGS

We remark that in [3], we use equation (8) in Maple to derive the orthotomic curves and surfaces for a given curve or surface. We shall describe how we can arrive the same conclusion by using **geometric constructions** using a DGS. We start with the case in 2D.

1. We refer readers to Figure 9(a). Assume we are given a parabolic curve C of the form $[t, at^2]$, where the parameter a can be input by user, and we start with a light source at P.

2. We pick a point A on C and construct the perpendicular to the tangent line at P, which is shown as A' in Figure 9(a). The locus of A' is called the pedal curve of C.

3. We construct A'' with the equation of $PA'' = 2PA'$, which is consistent with our earlier observation of $\mathbf{v} = \mathbf{v}_{\perp P} + \mathbf{v}_{\parallel P} = \mathbf{v} - 2\mathbf{v}_{\perp P}$. The locus of A'' is the orthotomic curve of C.

While visiting Chinese Academy of Sciences in Beijing in September of 2013, a student asked this question: If we are given an orthotomic or caustic curve, are we able to identify the light source and the original curve. After exploring the Java applet [7], see Figure 9(c), the answer is affirmative. We now move to the case in 3D.

1. We start with an ellipsoid S of the form $\frac{x^2}{a^2} + \frac{y^2}{b^2} + \frac{z^2}{c^2} = 1$ (seen as yellow in Figure 10 (a)), where the constants a, b, and c can be adjusted by users, and we start with a light source at A.

2. We pick a point B on the ellipsoid S (see Figure 10(a)) and construct the perpendicular to the tangent plane at B, which is shown as C in Figure 10(a). The locus of C is called the pedal surface (as seen in purple in Figure 10 (a)) for the ellipsoid. With the DGS, we can verify that AC is perpendicular to the tangent plane or parallel to the normal of the tangent plane.

3. We construct D by using $AD = 2AC$, which is again consistent with our earlier observation of $\mathbf{v} = \mathbf{v}_{\perp P} + \mathbf{v}_{\parallel P} = \mathbf{v} - 2\mathbf{v}_{\perp P}$. The locus of D is the orthotomic surface for the ellipsoid (as seen in green in Figure 10(b)).

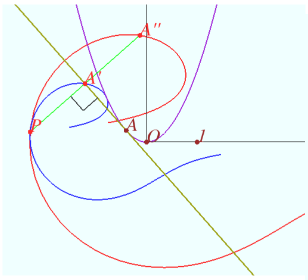

Figure 9(a) Orthotomic for a parabola

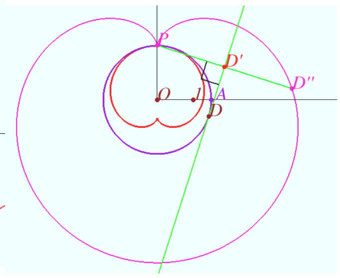

Figure 9(b) Orthotomic and caustic curves for a circle

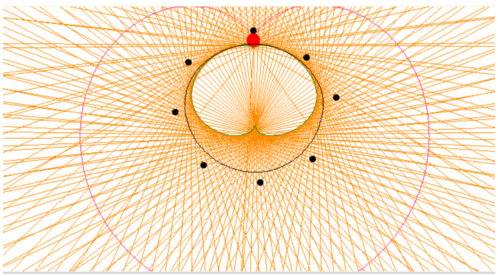

Figure 9(c) Evolute of orthotomic

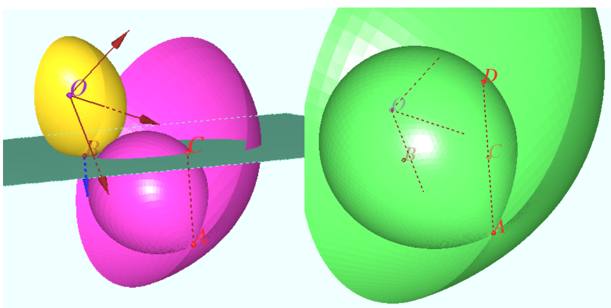

Figures 10(a) and (b) Pedal (purple) and Orthotomic (green) surfaces with respect to an ellipsoid (yellow)

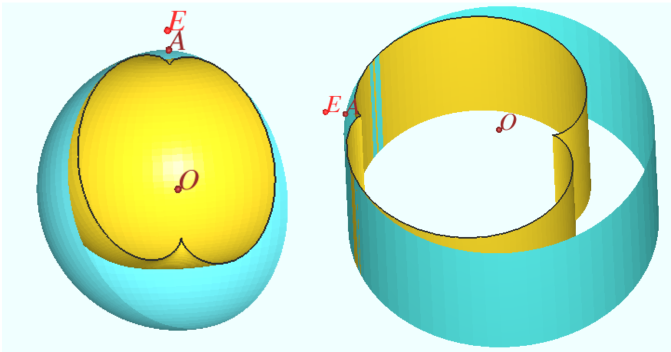

Figures 11(a) Caustic surface by rotation 11 (b) Caustic surface by shifting

We remark that the caustic curves in 2D can be defined explicitly if the light source is known and the equation of the original curve is defined. However, it is non-trivial to describe a caustic surface in 3D. We describe here how to find the caustic surfaces with respective to a symmetry surface such as a sphere or a cylinder. We further assume the light source is on the line of symmetry. In such case, we apply *rotation* (see Figure 11(a)) and *shifting* (see Figure 11(b)) techniques to obtain the corresponding caustic surfaces. We observe the following

Remarks:

- If we place the light source F near the edge of the sphere and the light source is placed along the line of symmetry as seen in Figure 11(a), the caustic surface will be rotating a 2D caustic curve (which is similar to the one in Figure 9(c)) around the line of symmetry.
- If we place the light source F near the edge of a cylinder and the light source is placed along the line of symmetry as seen in Figure 11(b), the caustic surface will be the vertical extensions from a 2D caustic curve (which is similar to the one in Figure 9(c)) along the center of the circle.

Caustic surfaces are important field for optics area. Thus we hope future integration of CAS and 3D DGS can inspire more collaborative works in cross disciplinary areas.

In general, computer software packages allow learners to explore complicated visualizations in 3D. Once we comprehend the concepts in 3D, we can extend our observations or results to finite dimensions when possible, and some of which can be extended to abstract spaces.

6 Conclusion

With current technological tools, an applied mathematics problem or project can be explored from different perspectives. We can ask if a solution exists; if it exists, how to approximate such solution. Do we use analytical answer or numerical answer before incorporating it into a DGS? What is the most efficient way of getting the answer? Finally, what are the real-life applications? Therefore, educators and researchers from all disciplines should work cooperatively to design proper set of projects for students to explore in different levels, from middle school to university and beyond. Consequently, new concepts or knowledge learned from exploration can be acquired naturally when students move from one level to the other. Author believes that mathematics knowledge gained through exploration will stay with learners for life. On the other hand, knowledge gained from preparing for an examination may last only briefly. Everyone will agree that examination is one way but not the only way to measure students' understandings. Technology becomes a bridge to make us rethink how to make mathematics an interesting and a cross disciplinary subject. Through the advancement of technological tools, learners will be able to discover more mathematics and its applications.

7 Acknowledgements

I would like to thank Professor Qun Lin, the State Key Laboratory of Scientific and Engineering Computing, Chinese Academy of Sciences, for providing me opportunities to give a series of lectures during September of 2013. This paper is partly derived from discussions with colleagues and students while visiting there.

References

[1] V. V. Shelomovskii and W.-C. Yang, *Finding volumes between a quadric surface and a plane*, the Electronic Journal of Mathematics and Technology (eJMT), Volume 7, Number 1, ISSN 1933–2823, Mathematics and Technology LLC.

[2] W.-C. Yang and V. V. Shelomovskii, *Mean Value Theorems in Higher Dimensions and Their Applications,* the Electronic Journal of Mathematics and Technology (eJMT), Volume 6, Number 1, ISSN 1933–2823, Mathematics and Technology LLC.

[3] W.-C. and M.-L. Lo, *General Inverses in 2-D, 3-D, applications inspired by Technology*, the Electronic Journal of Mathematics and Technology (eJMT), Volume 2, Number 3, ISSN 1933-2823, Mathematics and Technology LLC.

[4] W.-C. and M.-L. Lo, *Finding signed Areas and Volumes inspired by Technology*, the Electronic Journal of Mathematics and Technology (eJMT), Volume 2, Number 2, ISSN 1933-2823, Mathematics and Technology LLC.

[5] W.-C. Yang, *Some Geometric Interpretations of The Total Distances Among Curves and Surfaces*, the Electronic Journal of Mathematics and Technology (eJMT), Volume 3, Number 1, ISSN 1933-2823, Mathematics and Technology LLC.

[6] W.-C. Yang, *Revisit Mean Value, Cauchy Mean Value and Lagrange Remainder Theorems*, the Electronic Journal of Mathematics and Technology (eJMT), Volume 2, Number 2, ISSN 1933-2823, Mathematics and Technology LLC.

[7] A java applet, *Curve Simulator*, contributed by Shin Yoshizawa of Japan, posted at eJMT (http://ejmt.mathandtech.org) online resource section, https://php.radford.edu/~ejmt/Resources/CurveSimulator/CurveSimulator.html.

[8] GInMA: A Dynamic Geometry System, see http://deoma-cmd.ru/en/Products/Geometry/GInMA.aspx.

[9] Maple: A product of Maplesoft, see http://maplesoft.com/.

[10] Mathematica: A product of Wolfram Research, see http://www.wolfram.com/mathematica/.

[11] Geometer SketchPad: A Dynamic Geometry System, part of McGraw Hill education company, see http://www.keycurriculum.com/products/sketchpad.

[12] Cabri II: A Dynamic Geometry System, a product of Cabrilog, see http://www.cabri.com/.